The 3rd Asia-Pacific Solar Physics Meeting
Seoul National University, Korea
3 November 2015

A New Method for Coronal Magnetic Field Reconstruction

Sibaek Yi[1], G. S. Choe[1,2] & Daye Lim[1]

[1]School of Space Research, Kyung Hee University
Yongin, Korea

[2]Kyung Hee Astronomical Observatory, Kyung Hee University
Yongin, Korea

Coronal Magnetic Field Reconstruction

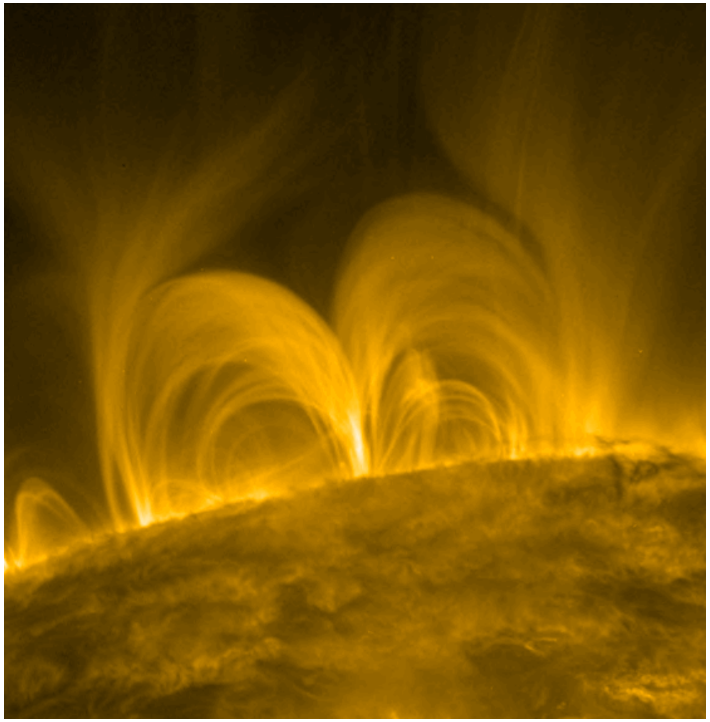

EUV observation by SDO AIA

- Coronal magnetic fields are difficult to measure.
- We need to reconstruct co ronal magnetic fields base d on vector-magnetogram data in the photosphere.

Force-Free Field Approximation

$$\mathbf{J}\times\mathbf{B}=\nabla p+\rho\mathbf{g}$$

For $\beta\ll 1$, and $|\mathbf{J}\times\mathbf{B}|\gg\rho\mathbf{g}$,

$$\mathbf{J}\times\mathbf{B}\approx 0$$
$$\mathbf{J}=\nabla\times\mathbf{B}=\alpha(\mathbf{r})\mathbf{B}$$

For well-posedness of the problem, B_n and J_n should be given at the boundaries, nothing more (Grad and Rubin 1958).

There Is No Extrapolation, but Reconstruction.

Can we extrapolate the FFF from the solar surface upward as Wu et al. (1990) proposed?

$$\frac{\partial B_x}{\partial z} = \alpha B_y + \frac{\partial B_z}{\partial x} ,$$

$$\frac{\partial B_y}{\partial z} = -\alpha B_x + \frac{\partial B_z}{\partial y} ,$$

$$\frac{\partial B_z}{\partial z} = -\frac{\partial B_x}{\partial x} - \frac{\partial B_y}{\partial y} ,$$

$$\alpha = \frac{1}{B_z}\left(\frac{\partial B_y}{\partial x} - \frac{\partial B_x}{\partial y}\right) ,$$

$$\frac{\partial(\alpha B_z)}{\partial z} = \frac{\partial}{\partial x}\left(\frac{\partial B_y}{\partial z}\right) - \frac{\partial}{\partial y}\left(\frac{\partial B_x}{\partial z}\right) .$$

- An ill-posed problem like solving a Laplace equation with both Dirichlet and Neumann conditions only in a part of the boundary.
- An arbitrarily small error can exponentially grow with *z*.

Reconstruction Methods

1. Non-variational method

- Grad-Rubin methods

  (Grad and Rubin 1958, Sakurai 1981, Amari et al. 1997, Wheatland 2004)

$\mathbf{B}^0$ assumed

$\rightarrow$ $\mathbf{J}^1$ loaded so that $\mathbf{J}^1 = \alpha(x_0, y_0)\mathbf{B}^0$

$\rightarrow$ $\mathbf{B}^1$ obtained by $\nabla\times\mathbf{B}^1 = \mathbf{J}^1$

Reconstruction Methods

2. Variational method

$$dW/dt = -\int_V \mathbf{F}\cdot\mathbf{v}\, dV < 0 \quad for \quad \mathbf{F}\cdot\mathbf{v} > \mathbf{0}$$

- Optimization methods (so far the best)
  (Wheatland et al. 2000, Wiegelmann 2004)

$$L = \int_V \left[|\mathbf{J}\times\mathbf{B}|^2 / B^2 + |\nabla\cdot\mathbf{B}|^2 \right] dV$$

- Viscous MHD relaxation method (VMRM) (Inoue et al. 2013, 2014)

Algorithm of Our Method

$\mathbf{B} = \nabla \times \mathbf{A}$

$$\partial \mathbf{A} / \partial t = -\mathbf{J}_{\perp}$$
$$= (\mathbf{J} \times \mathbf{B}) \times \mathbf{B} / B^2$$

In our method, $\nabla \cdot \mathbf{B}$ is naturally and exactly zero.

Implementation of Boundary Conditions

At the bottom boundary, imposing $\nabla \cdot \mathbf{A}_{xy} = 0$,

$\mathbf{A}_{xy} = z \times \nabla \phi$.

Therefore,

$\nabla_{xy}^2 \phi = B_z$

and

$\nabla_{xy}^2 A_z = -J_z$

$\rightarrow A_x , A_y$

$\rightarrow A_z$

Nested Grid System and Boundary Conditions

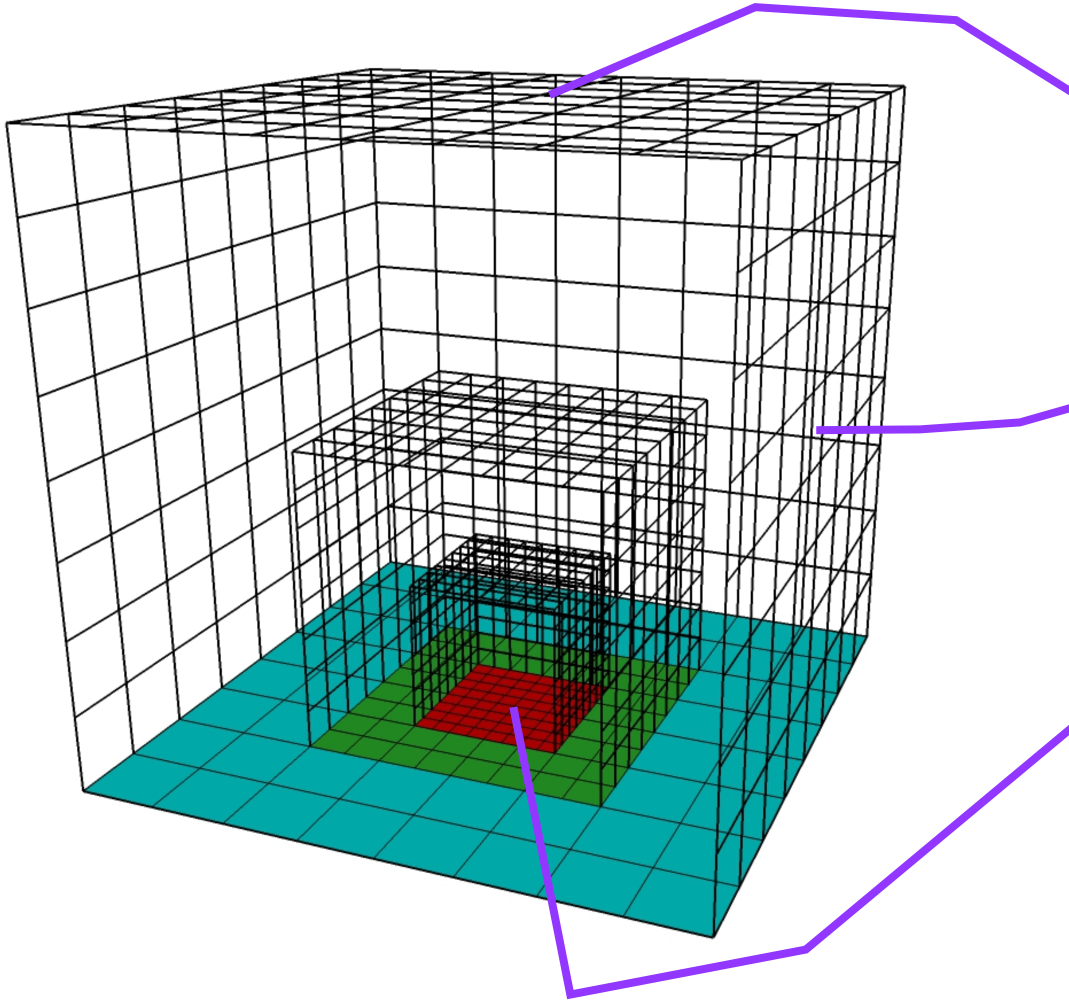

Source surface

Conducting slip-wall

and are fixe
d

Initial Condition – Current Preloaded

- Most FFF construction methods take a potential field as the initial condition.
- Then, current is initially located near the bottom boundary and gradually permeates the computational domain.
- In our initial condition, current is preloaded in the entire computational domain.
- For example,

  assuming $\nabla \times \boldsymbol{J}^0 = 0,\ \boldsymbol{J}^0 = \nabla\chi$.

  $\nabla \bullet \boldsymbol{J}^0 = 0 \Rightarrow$ Solving $\nabla^2\chi = 0$ gives $\boldsymbol{J}^0$.

  Our initial field is given by $\nabla \times \nabla \times \boldsymbol{A}^0 = \boldsymbol{J}^0$.

Numerical Methods for Approaching Equilibrium

$$dW/dt = -\int_V \mathbf{F}\cdot\mathbf{v}\, dV$$

1. Frictional method

$$\mathbf{v} = a\mathbf{F}$$

2. Gradient method

$$dt_n = a W_n\, dt_s / (W_n - W_s)$$

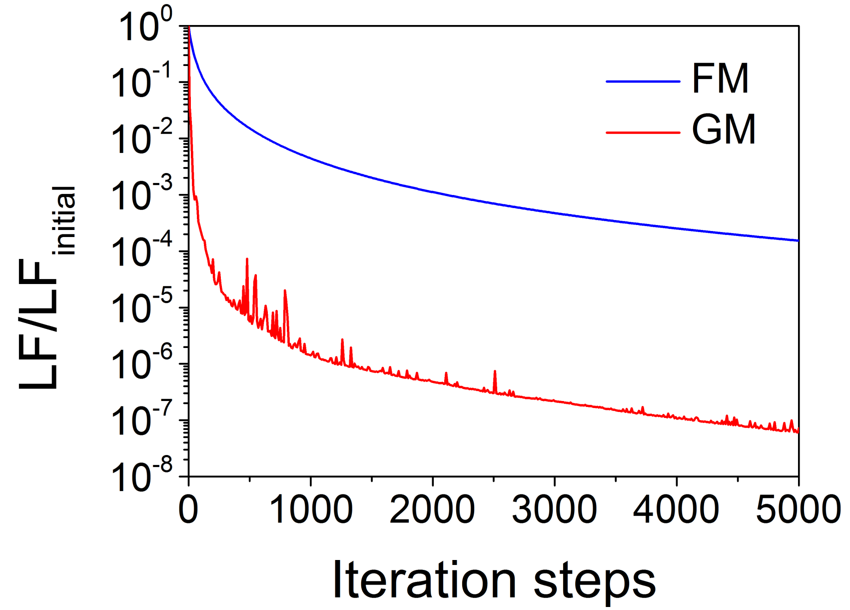

$$\mathrm{LF} = \int_V |\mathbf{J}\times\mathbf{B}|^2\, dV$$

Comparison of Convergence Rates

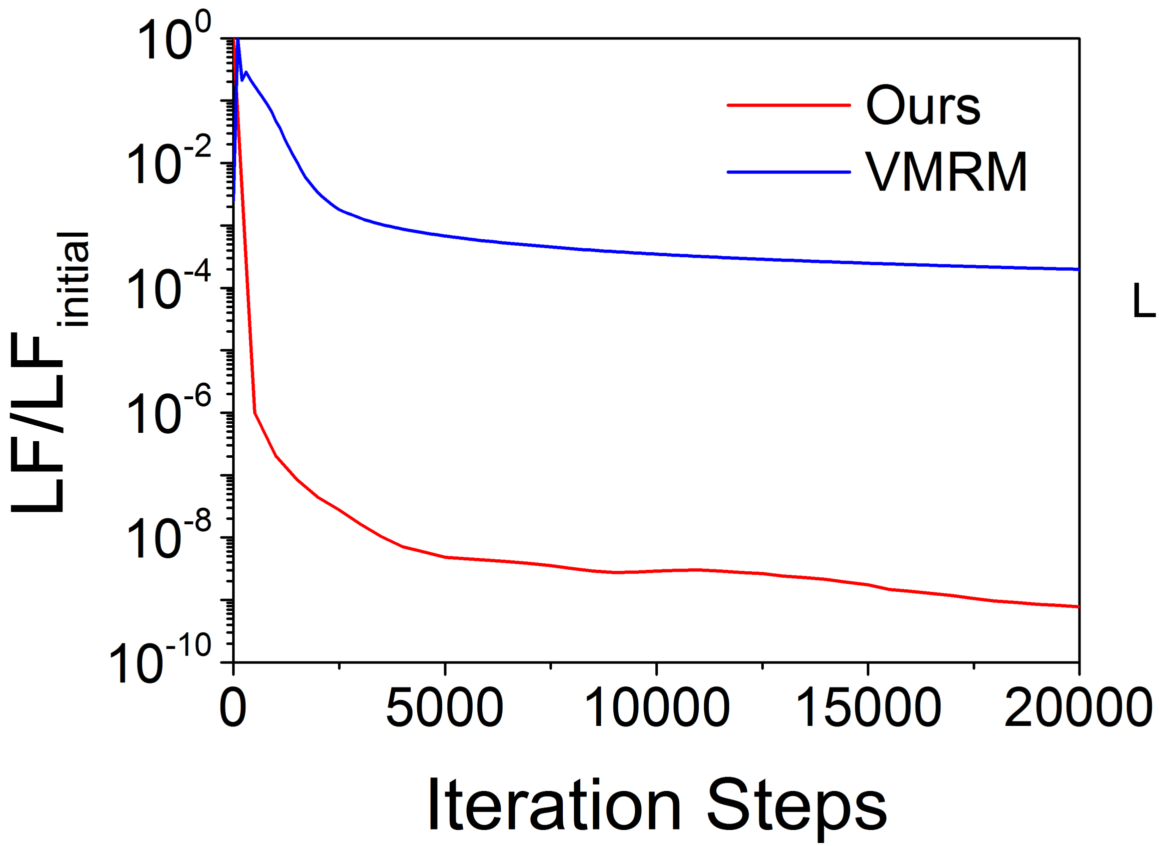

$$\mathrm{LF}=\int_V |\mathbf{J}\times\mathbf{B}|^2 \, dV$$

"Figures of Merits"
by Schrijver et al. (2006)

$$C_{vec} \equiv \sum_i \mathbf{B}_i \cdot \mathbf{b}_i \Big/ \sqrt{\sum_i |\mathbf{B}_i|^2 \sum_i |\mathbf{b}_i|^2} \qquad \equiv \left(\sum_i \frac{|\mathbf{j}_i \times \mathbf{b}_i|}{\mathbf{b}_i} \right) \Big/ \sum_i \mathbf{j}_i$$

$$C_{cs} \equiv \frac{1}{M} \sum_i \frac{\mathbf{B}_i \cdot \mathbf{b}_i}{|\mathbf{B}_i||\mathbf{b}_i|} \qquad L_f \equiv \frac{1}{V} \int_V \frac{|\mathbf{j} \times \mathbf{b}|^2}{\mathbf{b}^2} \, dV$$

$$E_n' = 1 - \sum_i |\mathbf{b}_i - \mathbf{B}_i| \Big/ \sum_i |\mathbf{B}_i|$$

$$E_m' = 1 - \frac{1}{M} \sum_i \frac{|\mathbf{b}_i - \mathbf{B}_i|}{|\mathbf{B}_i|}$$

$$\epsilon = \sum_i |\mathbf{b}_i|^2 \Big/ \sum_i |\mathbf{B}|^2$$

$\mathbf{b}_i$: Numerical solution
$\mathbf{B}_i$: Exact solution
M: Total number of grid points

Low and Lou Force-Free Field Model

Low and Lou (1990) presented a series of analytic solutions of the FFF equation

$$\frac{\partial^2 A}{\partial r^2} + \frac{1-\mu^2}{r^2}\frac{\partial^2 A}{\partial \mu^2} + Q\frac{dQ}{dA} = 0.$$

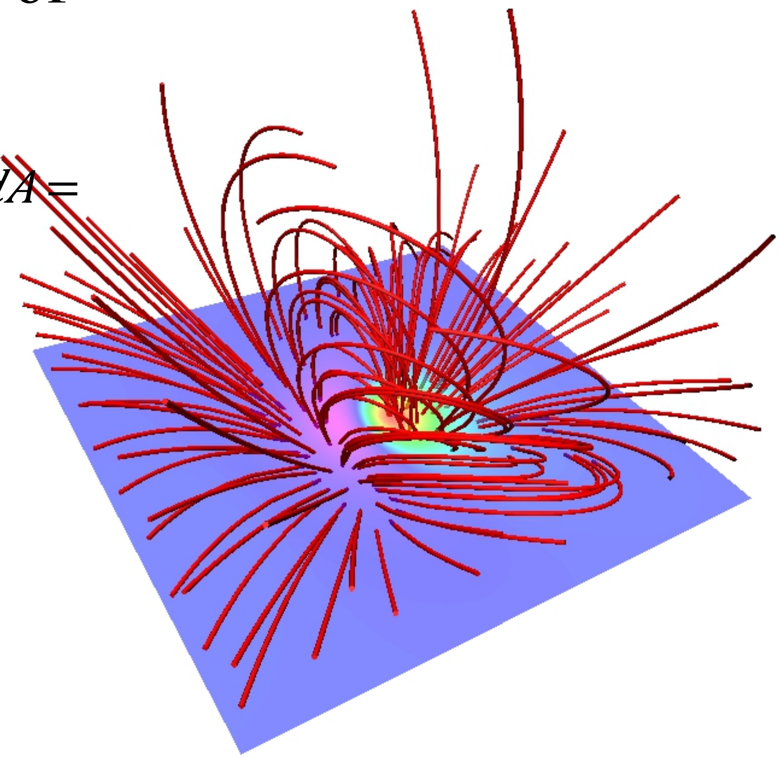

Using the ansatz,

$$A = \frac{P(\mu)}{r^n} \quad \text{and} \quad Q(A) = aA^{1+1/n},$$

we have a solvable equation:

$$(1-\mu^2)\frac{d^2 P}{d\mu} + n(n+1)P + a^2\frac{1+n}{n}P^{1+2/n} = 0.$$

Analytic Solution and Numerical Solution – Appearance Comparison

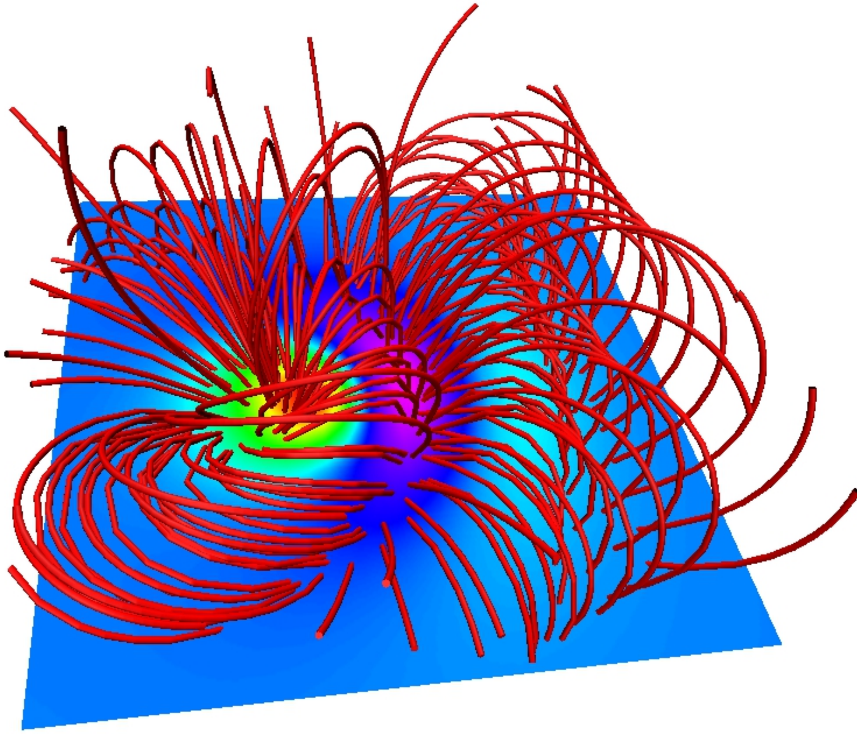

Low and Lou an alytic solution

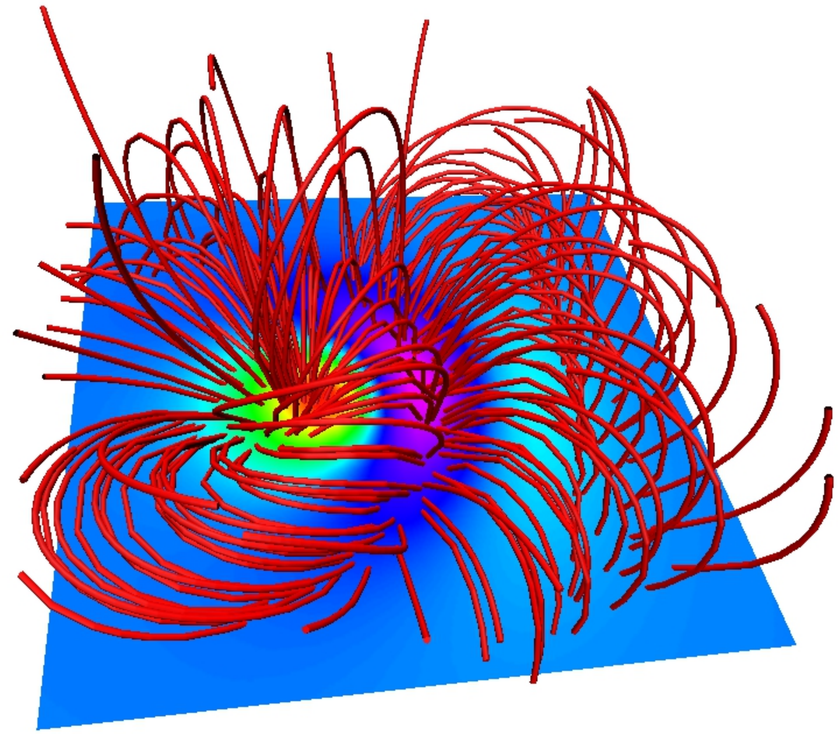

Our numerical solution

Two Test Cases in Schrijver et al. (2006)

◇ Case 1

- n=1, m=1, l=0.3, Φ=4/π
- 64^3 grid
- B_x, B_y, and B_z are given at all six boundaries (overspecified at all six boundaries).
- A non-practical situation.

◇ Case 2

- n=3, m=1, l=0.3, Φ=4/5π
- N^3 grid (N>64).
- Only **B** at z=0 is given (overspecified). We use only J_z.
- A practical situation.

Results of Two Different BC Settings

The same test as was done in Schrijver et al. (2006)

Model	C_{vec}	C_{cs}	E_{n}'	E_{m}'	ϵ	$\sigma(64^3)$	$L_f(64^3)$
Exact Solution	1	1	1	1	1	0	0
Case 1: B_x, B_y, and B_z are given at all six boundaries.							
Ours	1.00	0.98	0.88	0.80	0.98	$\mathbf{1.3\times10^{-4}}$	$\mathbf{1.2\times10^{-5}}$
Wiegelmann	1.00	1.00	0.97	0.96	1.02	$\mathbf{3.7\times10^{-2}}$	$\mathbf{1.9\times10^{-2}}$
Case 2: B_x, B_y, and B_z are given at the bottom boundary only.							
Ours	1.00	0.97	0.90	0.75	0.98	$\mathbf{4.2\times10^{-4}}$	$\mathbf{5.1\times10^{-4}}$
Wiegelmann	1.00	0.91	0.92	0.66	1.04	not given	not given

Flares in AR11974 on 2014 February 12

- GOES X-ray fluxes

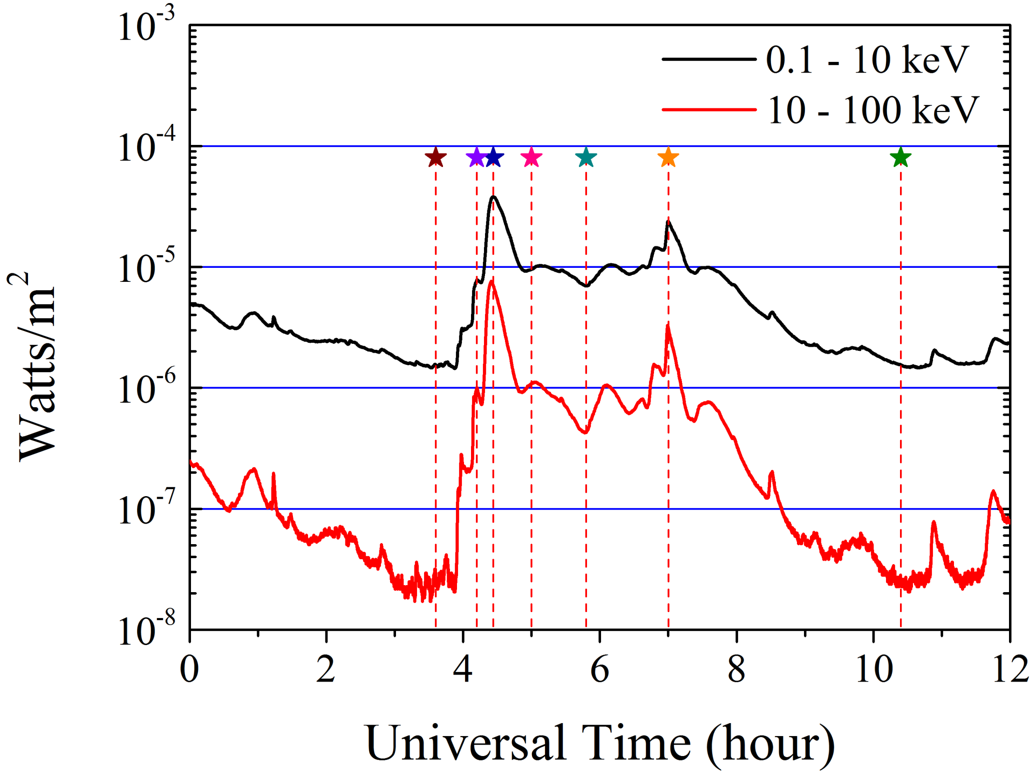

★ 02.12 UT 03:36:00

★ 02.12 UT 04:12:00

★ **02.12 UT 04:25:00 (M3.7)**

★ 02.12 UT 05:00:00

★ 02.12 UT 05:48:00

★ **02.12 UT 06:58:00 (M2.3)**

★ 02.12 UT 10:24:00

Reconstruction of the Magnetic Field in AR11974

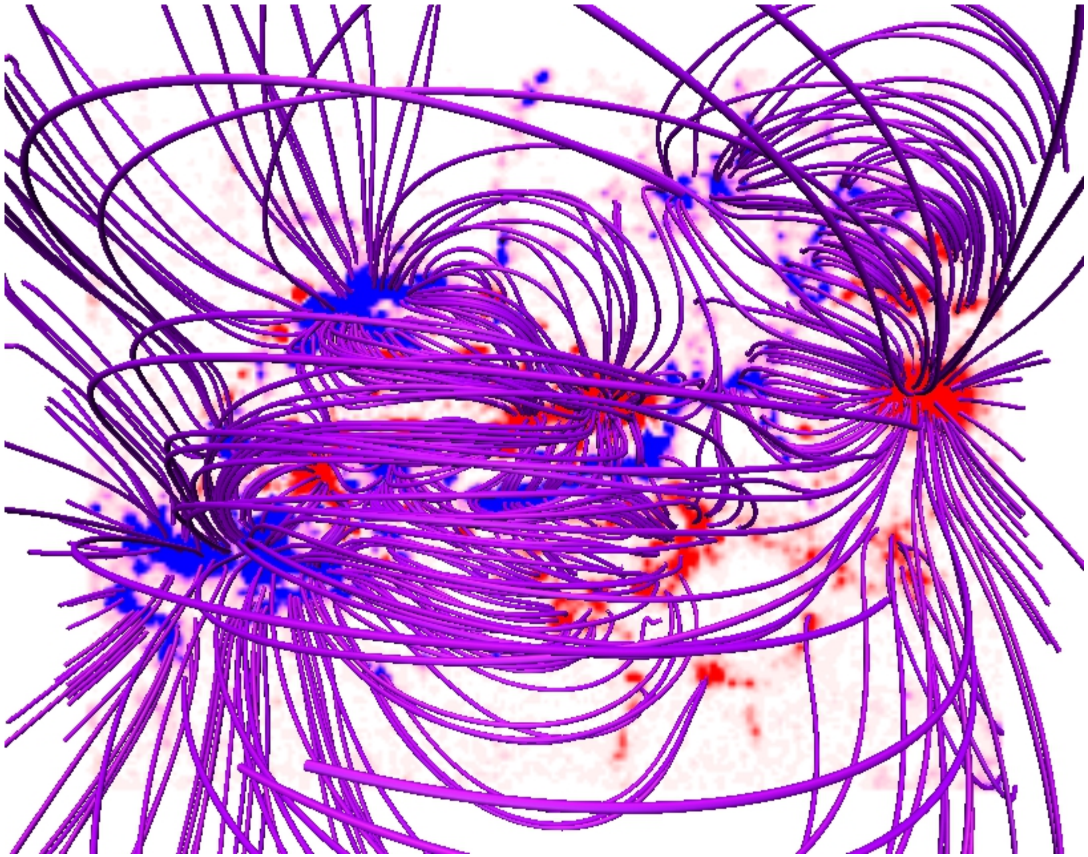

SDO AIA 171 Å

Reconstructed field lines

Magnetogram

2014 Feb. 12 03:36:00 UT

Sigmoid Structures in AR11974

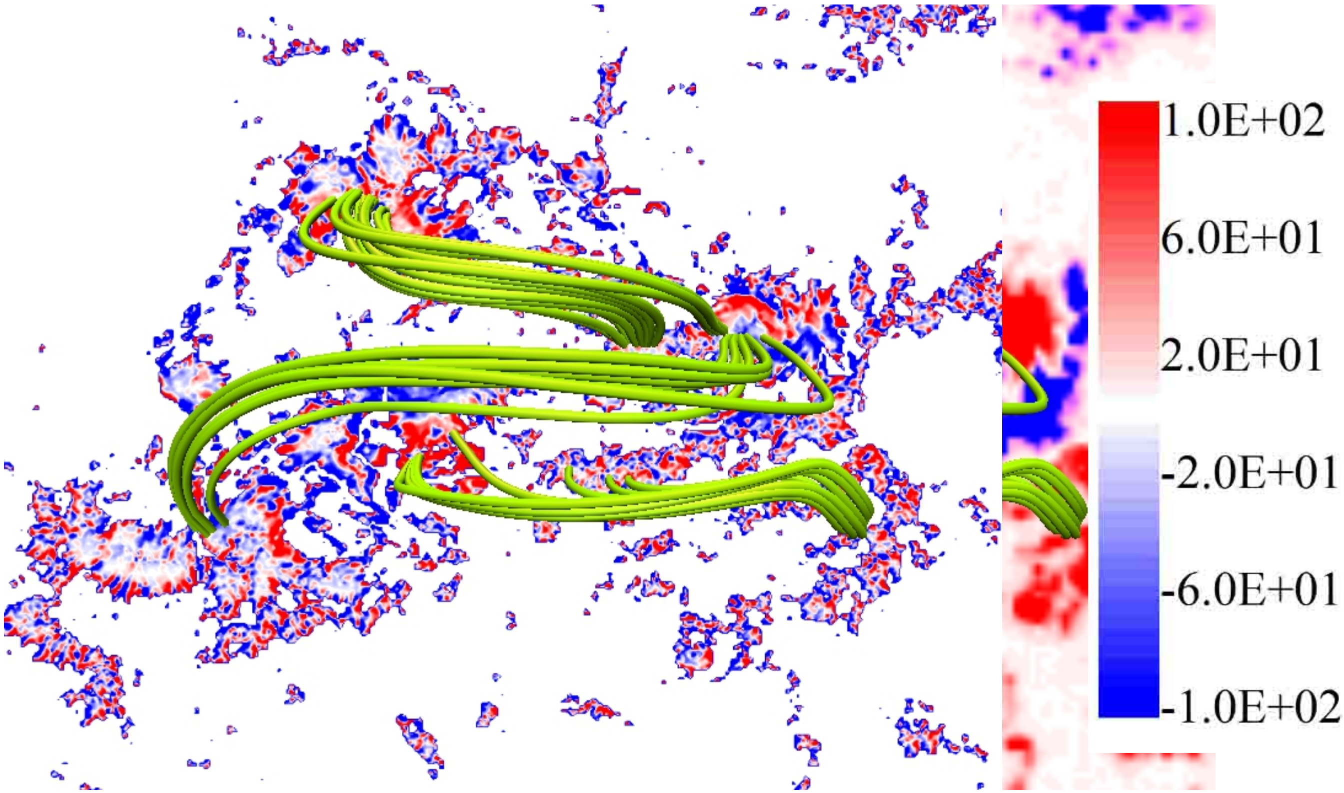

$\alpha=J_z/B_z$

One inverse-S-shaped and two S-shaped structures

Large Scale Eruption in AR11974

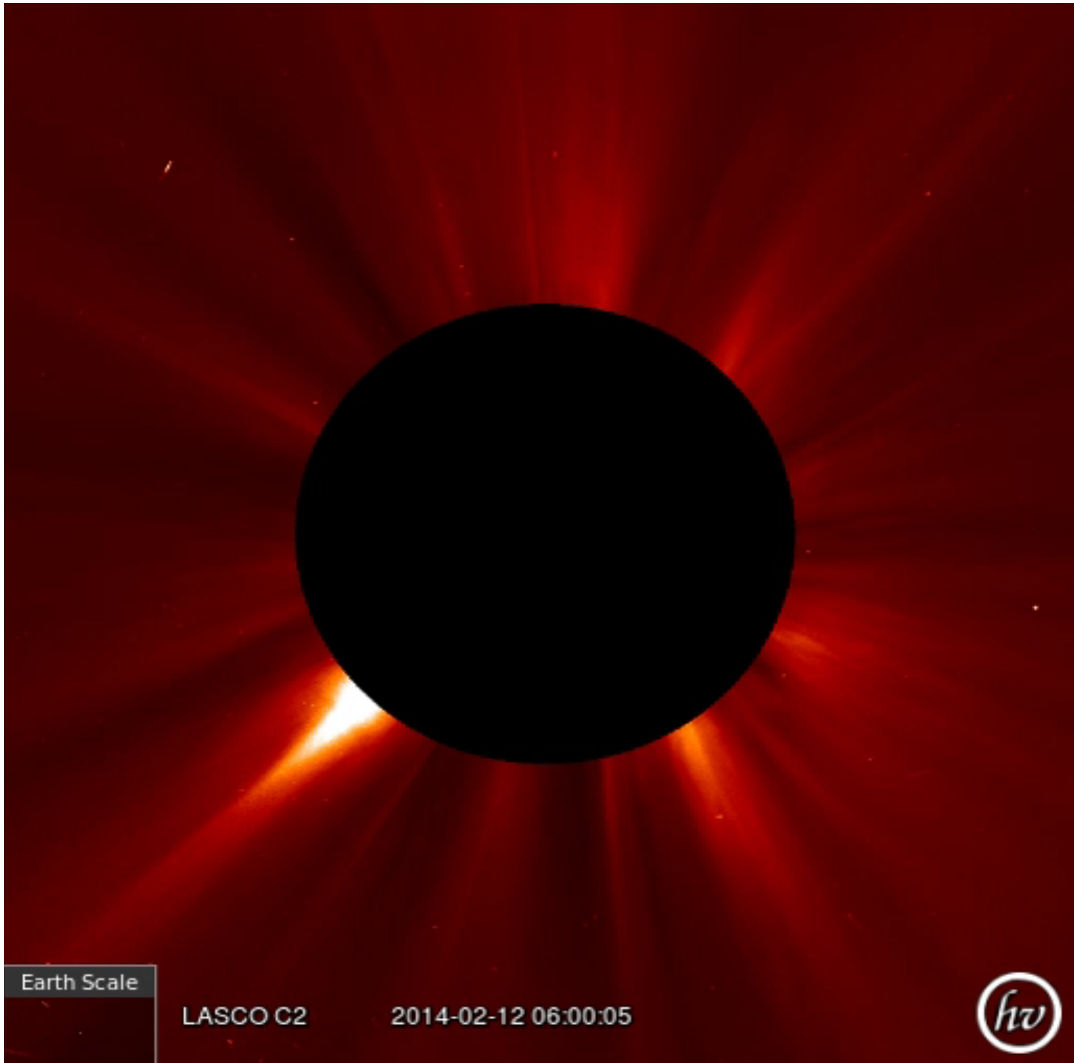

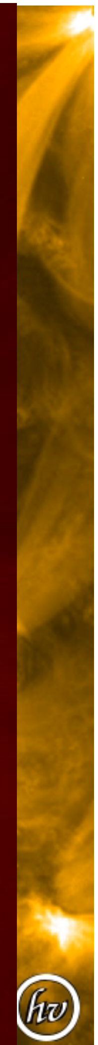

SOHO LASCO C2
CME observed at
06:00:05 UT

An erupting loop
at 04:35:00 UT

Two Interwound Flux Tubes

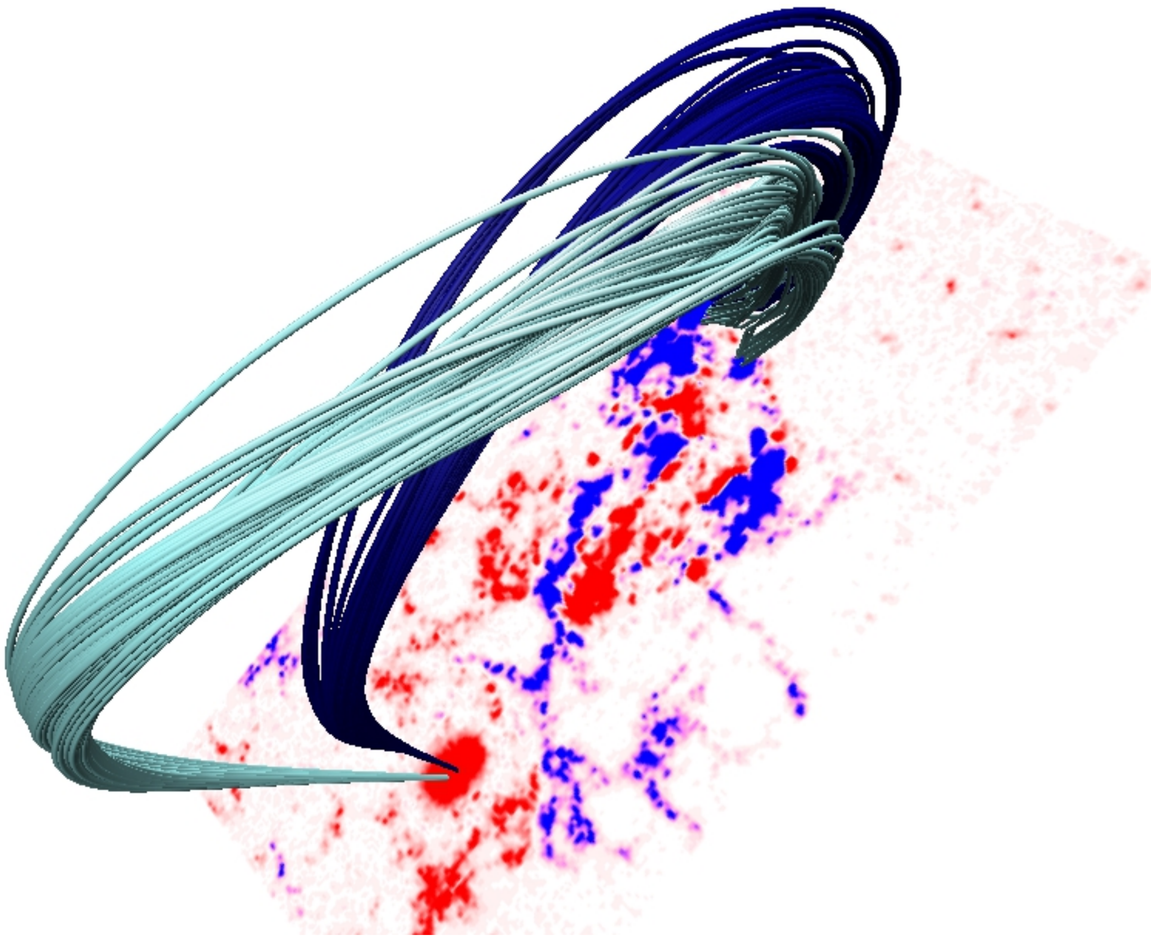

2014. 02. 12. 03:36:00 UT

Reconnection and Evolution of the Flux Tubes

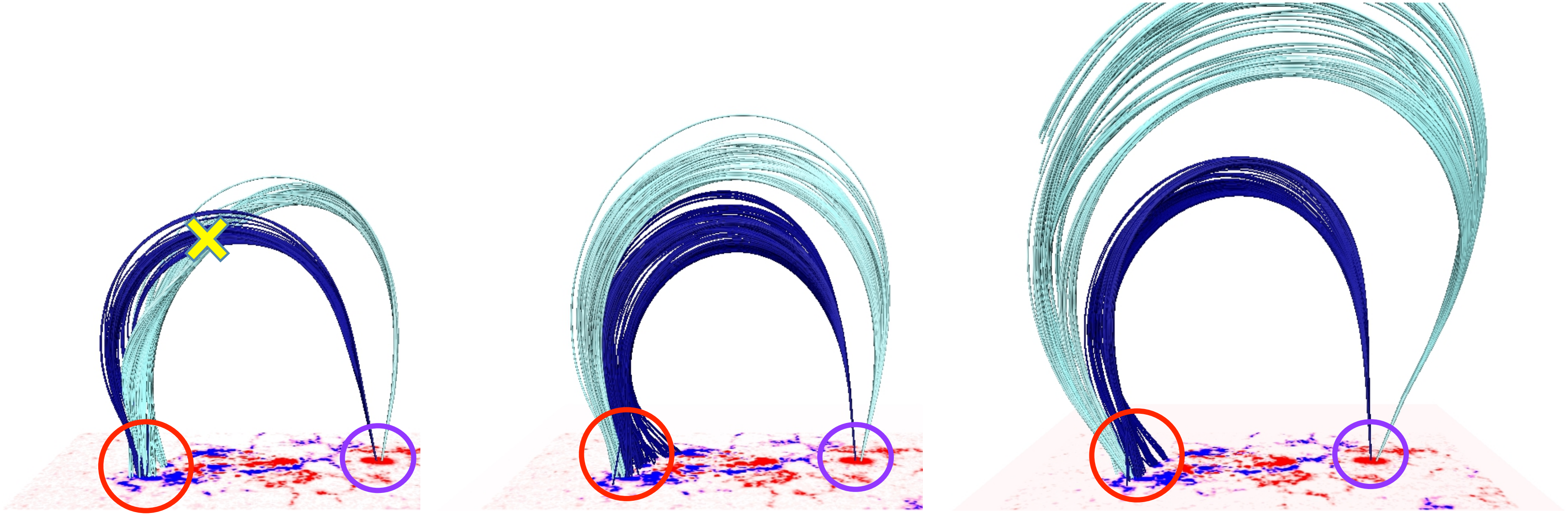

2014. 02. 12
. UT 03:36:0
0

2014. 02. 12
.
UT 05:48:00

2014. 02. 12
.
UT 10:24:00

Summary

- We have developed a new and efficient reconstr
  uction method for coronal FFFs.
- When only the bottom boundary data are given,
  our method excels in “figures of merits” by Sc
  hrijver et al. (2006).
- The reconstructed magnetic field in AR11974 s
  hows significant features of the eruption proces
  ses there.

Why Sigmoids are S-Shaped (Inverse-S-Shaped) for Positive α (Negative α)